Geophysical Research Letters

RESEARCH LETTER
10.1002/2018GL077328

Special Section:
New understanding of the solar eclipse effects on geospace: The 21 August 2017 Solar Eclipse

Suppression of the Polar Tongue of Ionization During the 21 August 2017 Solar Eclipse

Tong Dang[1], Jiuhou Lei[1], Wenbin Wang[2], Alan Burns[2], Binzheng Zhang[3,4], and Shun-Rong Zhang[5]

[1]CAS Key Laboratory of Geospace Environment, School of Earth and Space Sciences, University of Science and Technology of China, Hefei, China, [2]High Altitude Observatory, National Center for Atmospheric Research, Boulder, CO, USA, [3]Department of Earth Sciences, University of Hong Kong, Pokfulam, Hong Kong, [4]Laboratory for Space Research, University of Hong Kong, Pokfulam, Hong Kong, [5]MIT Haystack Observatory, Westford, MA, USA

Abstract It has long been recognized that during solar eclipses, the ionosphere-thermosphere system changes greatly within the eclipse shadow, due to the rapid reduction of solar irradiation. However, the concept that a solar eclipse impacts polar ionosphere behavior and dynamics as well as magnetosphere-ionosphere coupling has not been appreciated. In this study, we investigate the potential impact of the 21 August 2017 solar eclipse on the polar tongue of ionization (TOI) using a high-resolution, coupled ionosphere-thermosphere-electrodynamics model. The reduction of electron densities by the eclipse in the middle latitude TOI source region leads to a suppressed TOI in the polar region. The TOI suppression occurred when the solar eclipse moved into the afternoon sector. The Global Positioning System total electron content observations show similar tendency of polar region total electron content suppression. This study reveals that a solar eclipse occurring at middle latitudes may have significant influences on the polar ionosphere and magnetosphere-ionosphere coupling.

Plain Language Summary The ionosphere is the ionized part of Earth's upper atmosphere extending from about 60 to 1,000 km. During solar storm events, the dayside ionospheric plasma can be transported from middle latitude into the polar region by the electric field, leading to a "tongue-like" structure, which is called the "tongue of ionization (TOI)." Meanwhile, the solar eclipse can dramatically decrease the ionospheric plasma density within the Moon's shadow by the reduction of solar irradiation. Since the TOI structure is closely related to the middle latitude plasma density, it is interesting to explore the solar eclipse influences at middle latitudes on the polar ionospheric behavior associated with the polar TOI structure. On the basis of high-resolution simulations of the 21 August 2017 solar eclipse, it was reported that a significantly suppressed TOI occurred during the solar eclipse. The results provide new insights into the broad impacts of middle- and high- latitude eclipses on the behavior and dynamics of the high-latitude ionosphere and the geospace system.

Key Points:
- This is the first study of the TOI behavior at high latitudes during a solar eclipse using both model simulations and observations
- The TOI was strongly suppressed during the solar eclipse due to the reduction of electron density in the middle latitude source region
- The high-latitude ionospheric response to solar eclipses could have further effect on magnetosphere-ionosphere coupling

Correspondence to:
J. Lei,
leijh@ustc.edu.cn

Citation:
Dang, T., Lei, J., Wang, W., Burns, A., Zhang, B., & Zhang, S.-R. (2018). Suppression of the polar tongue of ionization during the 21 August 2017 solar eclipse. *Geophysical Research Letters*, *45*, 2918–2925. https://doi.org/10.1002/2018GL077328

Received 28 JAN 2018
Accepted 22 MAR 2018
Accepted article online 26 MAR 2018
Published online 13 APR 2018

1. Introduction

The tongue of ionization (TOI) is characterized by a longitudinally narrow region of enhanced plasma density moving antisunward from middle to high latitudes near the noon-midnight direction. The TOI is governed by polar convection electric fields, which transports dense plasma from the daytime midlatitudes into the polar cap region. Since they were first reported by Sato (1959) using maps of ground-based foF2, a number of studies have been carried out to investigate the TOI evolution and its dependence on universal time, season, and interplanetary magnetic field (e.g., David et al., 2016, Foster et al., 2005, Liu et al., 2017, Middleton et al., 2005, Thomas et al., 2013), during both major (e.g.Horvath & Lovell, 2015, Hosokawa et al., 2010, Liu et al., 2017) and weak (Liu et al., 2015) geomagnetic disturbances. These studies indicated that, besides the influence from the polar convection pattern, the TOI is also closely associated with plasma density variations at lower latitudes, that is, the TOI source region.

Solar eclipses can significantly decrease ionospheric electron density due to the rapid reduction of solar EUV irradiation (e.g., Anastassiadis & Matsoukas, 1969; Davis et al., 2000; Ding et al., 2010; Le et al., 2008; Müller-Wodarg et al., 1998; Salah et al., 1986). Therefore, it is interesting to explore solar eclipse influences on the TOI source region at middle and subauroral latitudes and to what degree these influences can propagate into the polar region, affecting the magnetosphere-ionosphere (M-I) coupling. Previous studies of the solar eclipse

effect on the ionosphere-thermosphere (I-T) system have mostly been concentrated on middle- and low-latitude effects; high-latitude ionospheric responses to solar eclipses have been rarely studied. A number of studies touched upon this issue using data from ionosondes (Davis et al., 2000), incoherent scatter radars (Baron & Hunsucker, 1973; Pitout et al., 2013), and total electron content (TEC) from the Global Positioning System (GPS) over some European stations (Krankowski et al., 2008). These studies, however, could not give a comprehensive view of the polar ionospheric responses to solar eclipses.

In this paper, we explore the solar eclipse effect on the polar TOI behavior during the recent 21 August 2017 solar eclipse, using the high-resolution Thermosphere Ionosphere Electrodynamics General Circulation Model (TIEGCM). In this study, the temporal evolution of the TOI and the polar ionosphere in different phases of the solar eclipse are examined. The results are also compared to GPS TEC observations.

2. Methodology

The National Center for Atmospheric Research TIEGCM self-consistently solves the coupled, nonlinear equations of momentum, energy, and continuity for neutral and ion species of the coupled global I-T system (Qian et al., 2014; Richmond et al., 1992; Roble et al., 1988). The newly developed high-resolution version of the TIEGCM is utilized in this study to simulate the physical processes of the I-T system at high latitudes impacted by the solar eclipse at mid and high latitudes. The high-resolution TIEGCM has a horizontal resolution of 0.625° × 0.625° in a geographic latitude-longitude grid and a vertical resolution of 1/4 scale height, which can better capture mesoscale structures in the I-T system, including those at high latitudes. The convection pattern at high latitudes is specified by the Heelis model (Heelis et al., 1982), which is driven by the *Kp* index. The precipitation in the TIEGCM includes electron precipitation, cusp precipitation, polar rain (drizzle), and ion precipitation. As the polar TOI can be transported through the cusp region, it should be mentioned that the cusp precipitation in the TIEGCM is parameterized by assuming a Gaussian distribution in both latitude and longitude.

The eclipse, which has also been called as the Great American Solar Eclipse, traversed the central continent of the United States from west to east. The total eclipse started over the east Pacific Ocean at 16:49 UT and ended over the North Atlantic Ocean at 20:02 UT. The penumbral shadow (partial eclipse) touched the Earth at 15:47 UT over the Pacific Ocean, covered a broad area of the North America, and disappeared at 21:04 UT. The calculation method of solar radiation changes caused by the eclipse in the TIEGCM is based on work by Curto et al. (2006) and Le et al. (2008). In this study, two TIEGCM simulations were conducted: one without and the other with the solar eclipse effect. The differential TECs between the two simulation runs were obtained to quantify the polar ionospheric changes during the 21 August 2017 solar eclipse.

Global Positioning System TEC data obtained from the MIT Madrigal Database were also utilized for verify comparison with simulation results. The TEC data were binned in a 2.5° × 2.5° grid in geographic longitude and latitude. The typical measurement error of TEC between 40° and 80° geographic latitudes on August 21 2017 was around 1 TECU. We calculated the difference between TEC values on 21 August 2017 and the monthly averaged ones in August 2017 to minimize the possible systemic bias. It should be pointed out that subtracting from the monthly averages cannot fully isolate the solar eclipse effect from the effect of ionospheric day-to-day variability and geomagnetic activity, but it does provide us some insights into the high-latitude ionospheric behavior during the solar eclipse.

3. Results

Figures 1a and 1b show the simulated distribution of TEC in the Northern Hemisphere at 19:27 UT on 21 August 2017 without and with the eclipse, respectively. In Figure 1a, at 19:27 UT, TEC was larger than 6 TEC units (TECU; 1 TECU = 10^{16} m^{-2}) at latitudes below 50°N on the dayside from 10 LT to 18 LT. Large TEC values are also seen in the latitude range of 60°N–70°N, which could be associated with auroral electron precipitation. The convection patterns are shown with the ionospheric electric potential as red (positive potential) and blue lines (negative potential) in Figure 1. The two-cell convection has a dawn cell of counter clock-wise circulation and a dusk cell of clockwise circulation. The plasma in the noon sector was transported antisunward into the polar cap by the ionospheric convection electric field. As a result, a TOI structure can be seen from the TEC enhancement at around 70°N at 12 LT. The TOI was evident in the narrow region at noon

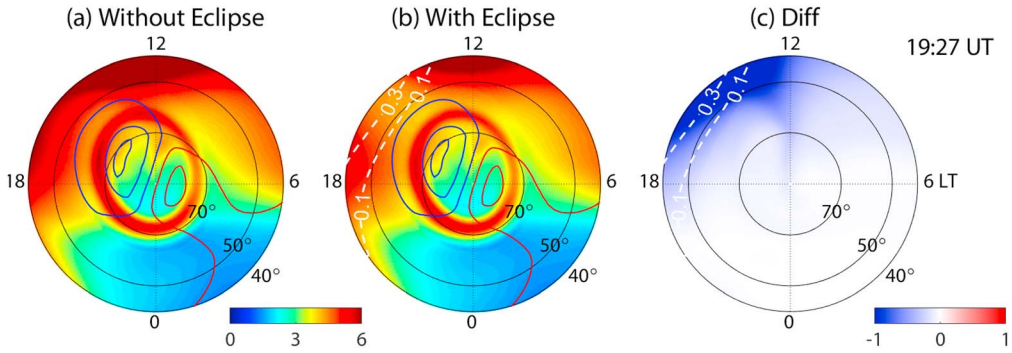

Figure 1. Polar maps of total electron content (TEC; units: TECU) in the Northern Hemisphere as a function of geographic latitude and local time from Thermosphere Ionosphere Electrodynamics General Circulation Model simulations (a) without and (b) with eclipse and (c) their difference (with eclipse-without eclipse) at 19:27 UT on 21 August 2017.

from 65°N near the auroral oval to around 80°N inside the polar cap region, with a magnitude of about 4 TECU.

Figure 1b shows the TEC distribution with the solar eclipse considered. The partial eclipse veiled a large part of the afternoon sector in the North America with obscuration rate indicated by the white dashed lines. The obscuration rate was 0.1 near 50°N and 0.4 at a geographic latitude of 40°N. Due to the reduction of ionization by the solar eclipse, the dayside electron density was decreased. As compared with the simulation result without eclipse, the TEC was reduced by 1–2 TECU, from local noon all the way to the dusk sector between 50°N and 70°N at this UT (Figure 1c). The simulated TOI appeared to be suppressed due to the eclipse-induced reduction of the source region electron density at the middle latitudes. The TEC near the auroral oval at about 14 LT was reduced by 1 TECU. Meanwhile, the TOI at around 70°N at 12 LT was decreased by 0.5 TECU. To further illustrate the suppression of TOI during the eclipse, Figure 1c depicts the distribution of the differential TEC between simulations with and without the eclipse. The contour plots were saturated to ±1 TECU to give a clear view of the TEC variation caused by the solar eclipse. It is obvious that the differential TEC exhibited a narrow "negative TOI" structure near the noon sector. The TEC suppression extended from the noon sector at around 55°N to the polar cap region. The TEC magnitude was reduced by more than 1 TECU at the middle latitude TOI source region and by 0.5 TECU in the TOI. This result indicates that the solar eclipse induced a decrease of electron density and TEC at middle latitudes, leading to the TOI suppression at high latitudes as less ionization was available for transport.

Figure 2 shows the differential TEC in local time and geographic latitude coordinates at five UTs during the 21 August 2017 solar eclipse. This figure further illustrates the evolution of TOI suppression during the solar eclipse. Note here that the differential TEC for GPS TEC was obtained by subtracting the monthly mean, whereas that for the simulation was the difference between model simulations with and without the eclipse. The GPS TEC showed negative perturbations in the most parts of the Northern Hemisphere and positive changes at high latitudes. This indicates a large day-to-day variability of the ionospheric TEC, which makes it difficult to isolate the pure influence of the solar eclipse from the observations. Therefore, we were mainly concentrating on the region that was impacted by the solar eclipse, as indicated by the obscuration rate (dashed lines) in the right panels of Figure 2. At 16:22 UT, the penumbra shadow started to cover the morning sector and the maximum latitude of the coverage was about 60°N. As shown in Figure 2a, TEC at latitudes lower than 50°N in the morning sector began to decrease, with a negative perturbation of about 1 TECU. For the TIEGCM simulation result shown in Figure 2b, TEC depletions could also be seen in the morning sector (from about 5 LT to 9 LT below 60°N), which was consistent with the observation.

At 16:47 UT, the partial eclipse moved more toward the polar region and the noon sector. The obscuration rate was close to 0.9 at 40°N at 6 LT, which is the perimeter latitude of the contour plot shown in Figure 2. It is clear that TEC depletions in both Figures 2c and 2d induced by the solar eclipse expanded to a geographic latitude of 65°N and a local time of 10 LT. Note that TEC depletions in the GPS data might be the mix of both ionospheric day-to-day variability and the eclipse effect, but the location and time of TEC depletions, as compared to the eclipse obscuration contours, give indication that those TEC depletions were, at least, partially due to the eclipse effects. The simulated differential TEC had a maximum depletion of

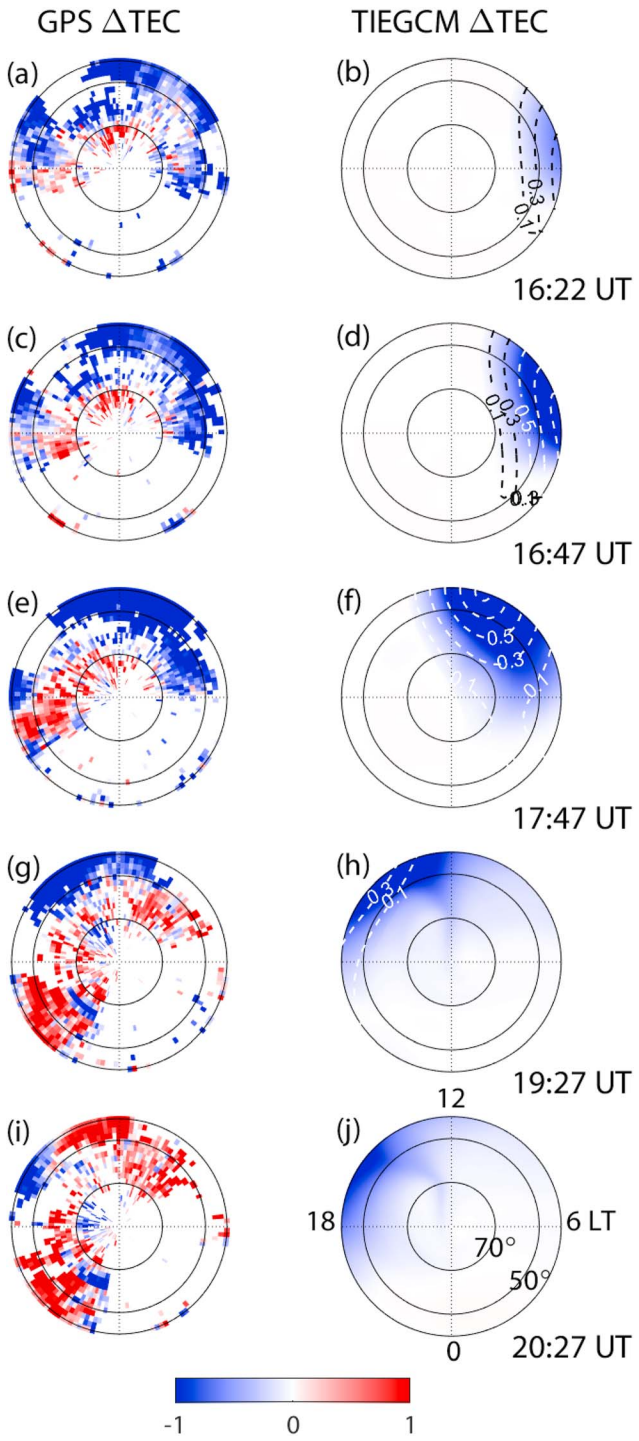

Figure 2. Polar maps of differential total electron content (TEC; units: TECU) in the Northern Hemisphere as a function of geographic latitude and local time from (left) Global Positioning System observations and (right) Thermosphere Ionosphere Electrodynamics General Circulation Model simulations on 21 August 2017. For the observation, the differential TEC maps represent the differences between TEC data on 21 August 2017 and the monthly average of August 2017; for the simulations, they were obtained from the simulations with and without eclipse (with eclipse-without eclipse). The dashed lines in the right panels indicate the obscuration rate of the solar eclipse at each UT.

greater than 1 TECU. An hour later at 17:47 UT, the penumbra path veiled almost all the morning sector. Both observations and simulations showed prominent TEC drops in most part of the morning sector, from middle latitudes all the way to the high latitude region (Figures 2e and 2f).

As time progressed, the partial eclipse moved to the afternoon sector (19:27 UT) and went farther away from the polar region. In Figures 2g and 2h, TECs were depleted mostly at latitudes lower than 50°N in the afternoon sector. Therefore, in the source region of the polar TOI structure, which is at middle latitudes in the afternoon sector, the ionization was greatly reduced by the solar eclipse. Consequently, the polar TOI structure, which is the result of plasma transport of ionization from the middle latitudes into the polar cap by the convection electric field, was also suppressed. As shown in Figure 2g, the GPS differential TEC showed a signature of TOI suppression of about 0.5–1.0 TECU, which extended from the middle latitudes at around 14 LT into the polar cap region. The simulated TOI suppression at 19:27 UT, which has been shown in Figure 1, appears to be consistent with the observation.

At 20:27 UT, the total eclipse had ended for 25 min and only a partial eclipse existed at low latitudes. There was no Moon shadow touching latitudes above 40°N. As shown in Figure 2i, in the afternoon sector, there was still a region of relatively depleted TEC in the GPS TEC data. This region aligned well with the eclipse-induced TEC depletion region shown in Figure 2j that was simulated by the model. This indicates that ionospheric perturbations induced by the solar eclipse did not recover and had a depletion of about 1 TECU at middle latitudes at this UT. A signature of a suppressed TOI can still be noted at around 15 LT between 50°N and 70°N. For the TIEGCM simulation result in Figure 2j, the TEC depletions covered a wide range of local time from local noon to about 21 LT. Compared to the observation in Figure 2i, the suppression of the TOI structure in Figure 2j was clearly seen, starting from about 15 LT at around 50°N to the polar cap region in the dusk sector.

Thus, our results in Figures 1 and 2 indicate that the TOI in the polar region was significantly suppressed by the 21 August 2017 solar eclipse through reducing the ionization in the source region at middle latitudes. Despite the fact that the totality of this solar eclipse occurred at middle and low latitudes, the TOI behavior and the polar ionosphere were affected by the solar eclipse.

4. Discussions and Summary

As shown in Figure 2, the GPS TEC showed positive or negative perturbations in the region far away from the solar eclipse, which was not obvious in the TIEGCM simulations. These perturbations might be related to ionospheric day-to-day variability and instantaneous geomagnetic activity. On the other hand, the TIEGCM results are the TEC differences between simulations with and without eclipse on the eclipse day (21 August 2017) and thus did not contain ionospheric day-to-day variability and were not affected greatly by the dynamic changes in high-latitude inputs of convection pattern and auroral precipitation associated with geomagnetic activity, as the TEC data were. Nevertheless, the large TEC depletion at middle latitudes in the afternoon sector and the associated suppression of the TOI structure at high latitudes are evident in the model results, and noticeable in observations, despite ionospheric day-to-day

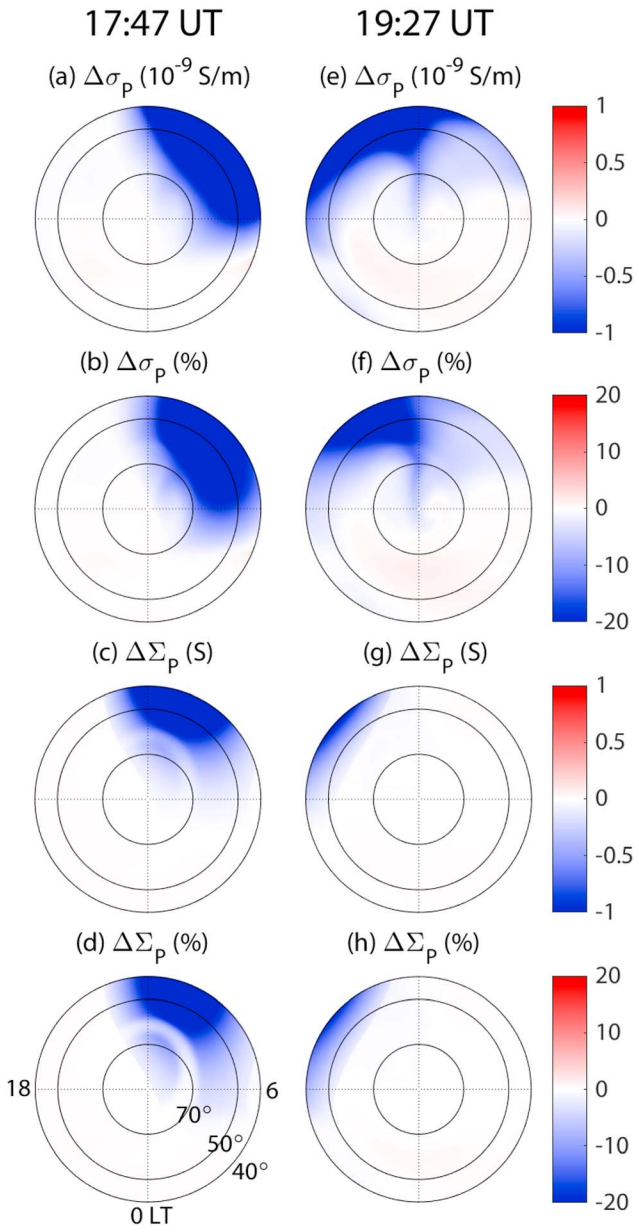

Figure 3. Polar maps of differential (a, b, e, and f) Pederson conductivity (σ_P) on Zp = 2 constant pressure surface (near the F_2 region peak) and (c, d, g, and h) height-integrated Pederson conductivity (Σ_P) in the Northern Hemisphere as a function of geographic latitude and local time at (left) 17:47 UT and (right) 19:27 UT on 21 August 2017. The differential σ_P and Σ_P are obtained from Thermosphere Ionosphere Electrodynamics General Circulation Model simulations with and without eclipse (with eclipse-without eclipse).

variability, lack of full data coverage, and dynamic changes in the high latitudes make it difficult to clearly identify the signature of the TOI suppression in data.

Most of the TOI reported in previous studies were related to the transport of plasma by the afternoon convection cell (e.g., Foster et al., 2005; Hosokawa et al., 2010). The dense plasma in the afternoon sector was more likely to be transported to the polar cap region by the convection electric field, as compared to the plasma in the morning sector (Figure 1). From the observations and our simulation results, the solar eclipse-induced suppression of the TOI would be more effective when the solar eclipse moved to the afternoon sector. In addition, the suppression of the TOI due to the solar eclipse is also dependent on geomagnetic activity. For this event, the *Kp* index was relatively low (around 2–3). It is expected that the "negative" TOI signature shown in Figure 2 would be more substantial if the eclipse coincided with the early hours of an intense geomagnetic storm, since middle latitude electron density is enhanced in storms and the storm time M-I convection tends to be stronger and can transport plasma from middle latitudes into the polar cap more effectively.

The above results show that a solar eclipse can reduce the electron density of a polar TOI, which is directly related to the middle and high-latitude ionospheric conductivity/conductance. Both the magnitude and spatial gradient of middle and high-latitude height-integrated ionospheric conductance play crucial roles in regulating the electrodynamic coupling between the magnetosphere and the ionosphere (e.g., Cowley, 2000; Ridley et al., 2004; Wang et al., 2004). As a consequence, the reduction of ionospheric electron density at both middle and high-latitudes due to the solar eclipse may have significant impact on the dynamics of the coupled solar wind-M-I system, by influencing the closure of magnetospheric currents at ionospheric altitudes with reduced ionospheric conductivity.

To further illustrate the solar eclipse effect on ionospheric conductivity, Figure 3 depicts the distributions of differential Pederson conductivity with and without the eclipse as a function of geographic latitude and local time. Figures 3a and 3b show the absolute difference and the percent difference of Pederson conductivity (σ_P) at the Zp = 2 constant pressure surface (near the F_2 region peak) at 17:47 UT. At this UT, the solar eclipse was in the morning sector and the Moon shadow of the partial eclipse extended into the polar region (dashed lines in Figure 2f). Corresponding to the TEC reduction in Figure 2f due to the reduction of solar irradiation caused by the solar eclipse, the Pederson conductivity in the ionospheric F_2 region exhibited a significant depletion in the morning sector as well. The largest reduction in the conductivity was greater than 20%. Figures 3c and 3d display similar polar maps but for the height-integrated Pederson conductivity (Σ_P), which is of critical importance in M-I coupling. We can note that a strong depletion of Σ_P occurring in the morning sector from middle latitudes to polar cap region. The Σ_P in the polar region decreased by around 0.2 S (Figure 3c) or 10% (Figure 3d). The large Σ_P change in the polar region was primarily related to the reduction of electron density and conductivity in the *E* region due directly to the solar eclipse, and thus, it shows obvious differences as compared with σ_P in the F_2 region (Figures 2a and 2b). This result indicates that the solar eclipse can greatly reduce the polar region ionospheric conductivity and thus influence the M-I coupling process. This effect can be greater if an eclipse happens at high middle latitudes or right over the auroral oval. The solar eclipse impact on the M-I coupling is also an interesting topic for the future work.

Figures 3e–3h show the corresponding results at 19:27 UT, when the solar eclipse moved into the afternoon sector and farther away from the polar region. As shown in Figures 3e and 3f, there was a great depletion of σ_P at middle latitudes in the afternoon sector and a "negative" tongue-like structure of σ_P, which was similar to the suppressed TOI in the TEC results as seen in Figures 1c and 2h. The σ_P within the "negative" tongue-like structure had an absolute depletion of about 0.5×10^{-9} S/m and a percent difference of around 10%. The height-integrated Pederson conductivity, however, did not show much change in the polar region, as displayed in Figures 2g and 2h. Σ_P perturbations were mainly located in the latitude range of 50°N and 70°N in the afternoon sector. On the eclipse day (21 August 2017), it was summer in the Northern Hemisphere and the daytime height-integrated ionospheric conductivity is dominated by the conductivity in the *E* region caused by the solar irradiation. Hence, the σ_P change within the "negative tongue" in the F_2 region, which was mainly associated with the plasma transport effect due to the convection electric field, makes only a small contribution to Σ_P and the possibly M-I coupling processes. However, the conductivity change within the "negative" tongue-like structure in the polar region still plays an important role in the ionospheric F_2 region dynamics. The ionospheric conductivity can directly influence local Joule heating and ion drag, which is crucial to the ion-neutral coupling process by changing the temperature, circulation, and composition of the thermosphere and dynamics and energetics within the I-T system. Thermospheric wind and density in the polar region has been reported to be strongly associated with Joule heating and ion drag (e.g., Sheng et al., 2015; Zhang et al., 2015); both are directly related to the magnitude of local ionospheric conductivity. In fact, Jee et al. (2007) showed that Joule heating rate per unit mass, which determines thermospheric temperature variations at high latitudes, increases with altitude. This makes it very important to understand the F_2 region electron density and conductivity changes for eclipses that occur at higher latitudes.

Depending on the latitude of the solar eclipse, at large scales ($>$200 km) the decrease of ionospheric electron density may cause significant changes in both the direction and magnitude of conductance gradient, which have already shown to be important for generating secondary electric fields in the ionosphere (e.g., Atkinson & Hutchison, 1978; Lotko et al., 2014). The induced electric fields, due to the changes in the gradient of Hall conductance during a solar eclipse, may have significant feedback effects on the configuration of magnetospheric convection, such as dawn-dusk asymmetries on the dayside and magnetospheric flow patterns on the nightside (e.g., Smith, 2012; Zhang et al., 2014). At meso- and small scales (e.g., 1 to 10 km), the decrease in Pedersen conductivity due to solar eclipse may have significant effects on the transmission, reflection, and resonance of magnetospheric Alfvén waves, which are important for both particle and electromagnetic energy deposition into the I-T system (Lysak, 1999; Lysak & Song, 2008; Streltsov & Lotko, 2004). Hence, solar eclipse events are not only interesting I-T "active experiments" for advancing understandings of the dynamics in the upper atmospheric system; they may also become important events for testing the hypotheses about the multiscale electrodynamic coupling within the whole geospace system. Further coordinated observational and theoretical studies are desired to explore the importance of solar eclipse events on the coupled geospace system, especially when future eclipse events occur at higher latitudes and during geomagnetically active periods. The 11 August 2018 partial eclipse with 0.73 magnitude over northern Europe and northeast Asia and the 10 June 2021 annual eclipse over northern Canada, Greenland, and Russia (see NASA Eclipse Site: https://eclipse.gsfc.nasa.gov/eclipse.html) are wonderful opportunities in the near future.

Note that this paper uses the TOI as an example to illustrate the potential effects of an eclipse occurring at higher latitudes on polar plasma transport. The high-latitude I-T system is very dynamic and complicated as it is directly under the influence of geomagnetic activity, making it very difficult to interpret the observational data, as shown in the case of GPS TEC data in Figure 2. Furthermore, an empirical high latitude ion convection model as used in this study does not necessarily represent the complexity of the actual plasma transport from subauroral to high latitudes which will determine the extension of the eclipse impact. Nevertheless, this paper clearly shows that eclipse-induced effects can have a significant effect on the high-latitude plasma distribution, dynamics in the I-T system, and electrodynamic coupling in all of geospace.

In summary, we have investigated the subauroral and polar region dynamical responses, as represented by the polar TOI, to the recent Great American Solar Eclipse using the high-resolution coupled thermosphere-ionosphere-electrodynamics model. The model shows an evident suppression of the TOI when an eclipse occurs in the afternoon sector at middle latitudes, due to the electron density reduction in the middle latitude source region. The GPS TEC data also show a similar signature of electron density suppression in the polar

region. These results provide us new insights into the broad impacts of middle- and high-latitude eclipses on the behavior and dynamics of the high-latitude ionosphere and the M-I coupling process.

Acknowledgments
The GPS TEC data are obtained by the MIT Haystack Observatory Madrigal database (http://www.openmadrigal.org). This work was supported by the National Natural Science Foundation of China (41325017 and 41421063), the Opening Funding of Chinese Academy of Sciences dedicated for the Chinese Meridian Project, and the Thousand Young Talents Program of China. The National Center for Atmospheric Research is sponsored by the National Science Foundation. We would like to acknowledge high-performance computing support from Cheyenne (https://doi.org/10.5065/D6RX99HX) provided by NCAR's Computational and Information Systems Laboratory, sponsored by the National Science Foundation (NSF). Simulation data, simulation codes, and analysis routines are being preserved on the NCAR High Performance Storage System and will be made available upon written request to the lead author.

References

Anastassiadis, M., & Matsoukas, D. (1969). Electron content measurements by beacon S-66 satellite during the May 20, 1966, solar eclipse. *Journal of Atmospheric and Terrestrial Physics*, *31*(9), 1217–1222. https://doi.org/10.1016/0021-9169(69)90056-7

Atkinson, G., & Hutchison, D. (1978). Effect of the day night ionospheric conductivity gradient on polar cap convective flow. *Journal of Geophysical Research*, *83*(A2), 725–729. https://doi.org/10.1029/JA083iA02p00725

Baron, M., & Hunsucker, R. (1973). Incoherent scatter radar observations of the auroral zone ionosphere during the total solar eclipse of July 10, 1972. *Journal of Geophysical Research*, *78*(31), 7451–7460. https://doi.org/10.1029/JA078i031p07451

Cowley, S. W. H. (2000). Magnetosphere-ionosphere interactions: A tutorial review. In *Magnetospheric current systems* (pp. 91–106). Washington, DC: American Geophysical Union. https://doi.org/10.1029/GM118p0091

Curto, J. J., Heilig, B., & Piñol, M. (2006). Modeling the geomagnetic effects caused by the solar eclipse of 11 August 1999. *Journal of Geophysical Research*, *111*, A07312. https://doi.org/10.1029/2005JA011499

David, M., Sojka, J. J., Schunk, R. W., & Coster, A. J. (2016). Polar cap patches and the tongue of ionization: A survey of GPS TEC maps from 2009 to 2015. *Geophysical Research Letters*, *43*, 2422–2428. https://doi.org/10.1002/2016GL068136

Davis, C. J., Lockwood, M., Bell, S. A., Smith, J. A., & Clarke, E. M. (2000). Ionospheric measurements of relative coronal brightness during the total solar eclipses of 11 August 1999 and 9 July 1945. *Annales de Geophysique*, *18*(2), 182–190. https://doi.org/10.1007/s00585-000-0182-z

Ding, F., Wan, W., Ning, B., Liu, L., le, H., Xu, G., et al. (2010). GPS TEC response to the 22 July 2009 total solar eclipse in East Asia. *Journal of Geophysical Research*, *115*, A07308. https://doi.org/10.1029/2009JA015113

Foster, J. C., Coster, A. J., Erickson, P. J., Holt, J. M., Lind, F. D., Rideout, W., et al. (2005). Multiradar observations of the polar tongue of ionization. *Journal of Geophysical Research*, *110*, A09S31. https://doi.org/10.1029/2004JA010928

Heelis, R. A., Lowell, J. K., & Spiro, R. W. (1982). A model of the high-latitude ionospheric convection pattern. *Journal of Geophysical Research*, *87*(A8), 6339–6345. https://doi.org/10.1029/JA087iA08p06339

Horvath, I., & Lovell, B. C. (2015). Storm-enhanced plasma density and polar tongue of ionization development during the 15 May 2005 superstorm. *Journal of Geophysical Research: Space Physics*, *120*, 5101–5116. https://doi.org/10.1002/2014JA020980

Hosokawa, K., Tsugawa, T., Shiokawa, K., Otsuka, Y., Nishitani, N., Ogawa, T., & Hairston, M. R. (2010). Dynamic temporal evolution of polar cap tongue of ionization during magnetic storm. *Journal of Geophysical Research*, *115*, A12333. https://doi.org/10.1029/2010JA015848

Jee, G., Burns, A. G., Wang, W., Solomon, S. C., Schunk, R. W., Scherliess, L., et al. (2007). Duration of an ionospheric data assimilation initialization of a coupled thermosphere-ionosphere model. *Space Weather*, *5*, S01004. https://doi.org/10.1029/2006SW000250

Krankowski, A., Shagimuratov, I. I., Baran, L. W., & Yakimova, G. A. (2008). The effect of total solar eclipse of October 3, 2005, on the total electron content over Europe. *Advances in Space Research*, *41*(4), 628–638. https://doi.org/10.1016/j.asr.2007.11.002

Le, H., Liu, L., Yue, X., & Wan, W. (2008). The midlatitude F2 layer during solar eclipses: Observations and modeling. *Journal of Geophysical Research*, *113*, A08309. https://doi.org/10.1029/2007JA013012

Liu, J., Nakamura, T., Liu, L., Wang, W., Balan, N., Nishiyama, T., et al. (2015). Formation of polar ionospheric tongue of ionization during minor geomagnetic disturbed conditions. *Journal of Geophysical Research: Space Physics*, *120*, 6860–6873. https://doi.org/10.1002/2015JA021393

Liu, J., Wang, W., Burns, A., Liu, L., & McInerney, J. (2017). A TIEGCM numerical study of the source and evolution of ionospheric F-region tongues of ionization: Universal time and interplanetary magnetic field dependence. *Journal of Atmospheric and Solar - Terrestrial Physics*, *156*, 87–96. https://doi.org/10.1016/j.jastp.2017.03.005

Lotko, W., Smith, R. H., Zhang, B. Z., Ouellette, J. E., Brambles, O. J., & Lyon, J. G. (2014). Ionospheric control of magnetotail reconnection. *Science*, *345*(6193), 184–187. https://doi.org/10.1126/science.1252907

Lysak, R. L. (1999). Propagation of Alfvén waves through the ionosphere: Dependence on ionospheric parameters. *Journal of Geophysical Research*, *104*(A5), 10,017–10,030. https://doi.org/10.1029/1999JA900024

Lysak, R. L., & Song, Y. (2008). Propagation of kinetic Alfvén waves in the ionospheric Alfvén resonator in the presence of density cavities. *Geophysical Research Letters*, *35*, L20101. https://doi.org/10.1029/2008GL035728

Middleton, H. R., Pryse, S. E., Kersley, L., Bust, G. S., Fremouw, E. J., Secan, J. A., & Denig, W. F. (2005). Evidence for the tongue of ionization under northward interplanetary magnetic field conditions. *Journal of Geophysical Research*, *110*, A07301. https://doi.org/10.1029/2004JA010800

Müller-Wodarg, I. C. F., Aylward, A. D., & Lockwood, M. (1998). Effects of a mid-latitude solar eclipse on the thermosphere and ionosphere—A modelling study. *Geophysical Research Letters*, *25*(20), 3787–3790. https://doi.org/10.1029/1998GL900045

Pitout, F., Blelly, P. L., & Alcaydé, D. (2013). High-latitude ionospheric response to the solar eclipse of 1 August 2008: EISCAT observations and TRANSCAR simulation. *Journal of Atmospheric and Solar - Terrestrial Physics*, *105-106*, 336–349. https://doi.org/10.1016/j.jastp.2013.02.004

Qian, L., Burns, A. G., Emery, B. A., Foster, B., Lu, G., Maute, A., et al. (2014). The NCAR TIE-GCM: A community model of the coupled thermosphere/ionosphere system. In J. D. Huba, R. W. Schunk, & G. Khazanov (Eds.), *Modeling the ionosphere-thermosphere system* (pp. 73–83). Washington, DC: American Geophysical Union. https://doi.org/10.1002/9781118704417.ch7

Richmond, A. D., Ridley, E. C., & Roble, R. G. (1992). A thermosphere/ionosphere general circulation model with coupled electrodynamics. *Geophysical Research Letters*, *19*(6), 601–604. https://doi.org/10.1029/92GL00401

Ridley, A. J., Gombosi, T. I., & DeZeeuw, D. L. (2004). Ionospheric control of the magnetosphere: Conductance. *Annales de Geophysique*, *22*(2), 567–584. https://doi.org/10.5194/angeo-22-567-2004

Roble, R. G., Ridley, E. C., Richmond, A. D., & Dickinson, R. E. (1988). A coupled thermosphere/ionosphere general circulation model. *Geophysical Research Letters*, *15*(12), 1325–1328. https://doi.org/10.1029/GL015i012p01325

Salah, J. E., Oliver, W. L., Foster, J. C., Holt, J. M., Emery, B. A., & Roble, R. G. (1986). Observations of the May 30, 1984, annular solar eclipse at Millstone Hill. *Journal of Geophysical Research*, *91*(A2), 1651–1660. https://doi.org/10.1029/JA091iA02p01651

Sato, T. (1959). Morphology of ionospheric F2 disturbances in the polar regions. *Report of Ionosphere and Space Research in Japan*, *13*, 91–95.

Sheng, C., Deng, Y., Wu, Q., Ridley, A., & Häggström, I. (2015). Thermospheric winds around the cusp region. *Journal of Geophysical Research: Space Physics*, *120*, 1248–1255. https://doi.org/10.1002/2014JA020028

Smith, R. (2012). Effects of ionospheric conductance on magnetosphere-ionosphere coupling, (MS thesis). Hanover, NH: Thayer School of Engineering, Dartmouth College.

Streltsov, A. V., & Lotko, W. (2004). Multiscale electrodynamics of the ionosphere-magnetosphere system. *Journal of Geophysical Research*, *109*, A09214. https://doi.org/10.1029/2004JA010457

Thomas, E. G., Baker, J. B. H., Ruohoniemi, J. M., Clausen, L. B. N., Coster, A. J., Foster, J. C., & Erickson, P. J. (2013). Direct observations of the role of convection electric field in the formation of a polar tongue of ionization from storm enhanced density. *Journal of Geophysical Research*, *118*, 1180–1189. https://doi.org/10.1002/jgra.50116

Wang, W., Wiltberger, M., Burns, A. G., Solomon, S. C., Killeen, T. L., Maruyama, N., & Lyon, J. G. (2004). Initial results from the coupled magnetosphere-ionosphere-thermosphere model: Thermosphere-ionosphere responses. *Journal of Atmospheric and Solar - Terrestrial Physics*, *66*(15-16), 1425–1441. https://doi.org/10.1016/j.jastp.2004.04.008

Zhang, B., Lotko, W., Brambles, O., Xi, S., Wiltberger, M., & Lyon, J. (2014). Solar wind control of auroral Alfvénic power generated in the magnetotail. *Journal of Geophysical Research: Space Physics*, *119*, 1734–1748. https://doi.org/10.1002/2013JA019178

Zhang, B., Varney, R. H., Lotko, W., Brambles, O. J., Wang, W., Lei, J., et al. (2015). Pathways of F region thermospheric mass density enhancement via soft electron precipitation. *Journal of Geophysical Research: Space Physics*, *120*, 5824–5831. https://doi.org/10.1002/2015JA020999